Enhanced hydrolysis of aluminium nitride from secondary aluminum dross through combination of wet-stirred milling and alkaline leaching

Qiang GUO (qguo@ipe.ac.cn)
CAS Institute of Process Engineering: Institute of Process Engineering Chinese Academy of Sciences
https://orcid.org/0000-0002-9184-1600

Huilin Li
Zhengzhou Institute of Emerging Industrial Technology

Mingbo Fu
Zhengzhou Institute of Emerging Industrial Technology

Yongli Li
CAS Institute of Process Engineering: Institute of Process Engineering Chinese Academy of Sciences

Dengchao Tian
Zhengzhou Institute of Emerging Industrial Technology

Ling Zhang
CAS Institute of Process Engineering: Institute of Process Engineering Chinese Academy of Sciences

Research Article

Keywords: Secondary aluminum dross, aluminium nitride hydrolysis, Wet-stirred milling, Alkaline leaching, kinetics analysis

Posted Date: September 14th, 2022

DOI: https://doi.org/10.21203/rs.3.rs-2012746/v1

Version of Record: A version of this preprint was published at Waste and Biomass Valorization on April 28th, 2023. See the published version at https://doi.org/10.1007/s12649-022-02020-4.

Abstract

Deep hydrolysis for removing hazardous aluminium nitride (AlN) from secondary aluminum dross (SAD) remains a challenge nowadays. Enhanced hydrolysis of AlN from SAD through a combination of wet-stirred milling and alkaline leaching is investigated in the present study, which has not been reported before. SAD is activated during wet-stirred milling just with water by reducing the grain size and increasing the active surface area. Leaching with NaOH dissolves the hydrolysis products (AlOOH, $Al(OH)_3$) to expose reactive sites of unhydrolyzed AlN, contributing to the enhanced hydrolysis process. Results indicate that by utilizing optimized conditions (10 min wet milling, 5 wt.% NaOH solution, L/S ratio of 2, 75 ℃ temperature, and 120 min duration), 98.3% of AlN is removed from SAD. The kinetic analysis indicates that the hydrolysis process is controlled by both diffusion and chemical reactions, with the activation energy calculated to be 31.0 kJ/mol. After undergoing this enhanced hydrolysis process, the residue, which consisted primarily of Al_2O_3 and $Al(OH)_3$,can be recycled as Al concentrate. The technology has been already applied in a pilot plant and achieved a favorable effect in practical applications.

Statement of Novelty

Efficient hydrolysis for removing hazardous aluminium nitride (AlN) from secondary aluminum dross (SAD) remains a challenge nowadays. An enhanced hydrolysis process for removing AlN from SAD has been developed and reported in this study. The results demonstrate that the progress is highly efficient and can be performed using a combination of wet-stirred milling and alkaline leaching. This solution has not been reported before, and relevant patent authorization has been obtained by our research group.

The technology has been already applied in a pilot plant that processes 20000 tons of SAD per year, achieving a favorable effect in practical applications, facilitating the disposal of waste and the protection of environment.

1. Introduction

Aluminum (Al) is widely used in various fields due to its inherent properties which include good elasticity, high specific strength and stiffness, high impact resistance, high anti-wear and anti-corrosion, high conductivity and good formability. Globally, the production of Al was estimated to be 65.3 million tons in 2020, with this figure growing annually (https://world-bureau.co.uk/).Al dross is the primary byproduct during production, with as much as 15–25 kg generated for every 100 kg of molten aluminum. This is rapidly becoming a significant source of environmental pollution as production increases worldwide [1].

Al dross is classified as either primary or secondary aluminum dross (SAD), dependent on the number of times Al is recovered and the residual metallic Al content [2]. The main constituents of SAD are metallic Al (5–10 wt.%), aluminum oxide (Al_2O_3, 20–50 wt.%), aluminum nitride (AlN, 10–20 wt.%), and various salt-flux (chlorides and fluorides) mixtures [3]. Hazardous components, like AlN, chlorides, and fluorides lead to serious environmental problems depending upon how waste material is handled [4]. A significant

environmental concern is the generation and release of NH_3 to the atmosphere, caused from the reaction between AlN and water ($AlN + 3H_2O = Al(OH)_3 + NH_3$). Consequently, SAD is classified as a hazardous waste and is restricted from disposal in landfills without undergoing any pre-treatment.

Over time, public concern has grown regarding the treatment and utilization of SAD. Various methods have been proposed for the recovery of alumina from SAD [5–8]. In addition, several products are manufactured for exclusive utilization of SAD, including building materials [9–12], refractories [13, 14], deoxidizers, molecular sieves [15–17] and compound flocculants [18]. The correct treatment of AlN is very important during these processes.

There several strategies have been devised for treatment of AlN present in SAD. This has focused on inhibition of the hydrolysis reaction to prevent evolution of ammonia. Li et al. investigated the leaching process of SAD using CO_2-saturated water [19]. The results indicated that formation of ammonia was significantly hindered, with a small quantity of NH_3 absorbed generating NH_4HCO_3 species. Nevertheless, this methodology for inhibiting ammonia formation at low pH could not completely eliminate the toxic by-products.

An alternative strategy is removing AlN from SAD through a hydrolysis reaction. Typically, hydrolysis reactions occur through four stages, namely induction, rapid hydrolysis and aggregation, aggregation balance with further reaction, and ripening [20]. Zhang reported the percentage of AlN hydrolysis from dross was only 40% as the hydrolysis reaction was controlled by diffusion [21]. Li studied the hydrolysis behavior of AlN present in SAD, reporting that the surface of AlN particles was coated with a hydrolytic layer [22]. This layer was characterized by the presence of an amorphous or poorly crystalline boehmite phase during leaching, with this proposed to inhibit the hydrolysis reaction.

The evolution of aluminum hydroxides from AlN suspended in dilute aqueous solution has also been studied. The first, short-lived, hydrolysis reaction product was an amorphous aluminum hydroxide gel ($Al(OH)_3(OH_2)$), which then transformed into AlOOH and $Al(OH)_3$ [23, 24]. These solid products are easy to generate and will agglomerate on the surface of AlN particles, hindering the reaction through passivating reactive sites of unhydrolyzed AlN.

Enhanced hydrolysis of AlN through a combination of wet-stirred milling and alkaline leaching is studied to determine a solution to this ongoing issue in this investigation. To the best of our knowledge, this solution has not been reported before, and relevant patent authorization has been obtained by our research group [25, 26]. Furthermore, the technology has been already applied in a pilot plant that processes 20000 tons of SAD per year in Henan province, China.

The whole process is schematically illustrated in Fig. 1. SAD is treated by wet-stirred milling just with water to reduce the grain size and increase the active contact area. During the milling process, NaCl, KCl, and NaF salts are dissolved so that they can be recycled. Following this the slurry is leached with alkaline solution. Given the strong reaction between alkaline solution and AlN, the hydrolysis products, which

include AlOOH and $Al(OH)_3$, can be separated from the surface of AlN particles. This allows the hydrolysis reaction to continue and achieve improved dissolution of AlN present. Consequently, the leachate can be recycled as a lixiviant, with the residue utilized as an Al concentrate.

2. Experimental

2.1 Raw materials

SAD was collected from an aluminum smelter in Henan province, China. Before performing all the experiments, SAD was dried at 100°C for 4 h, and then ground using jar mill for 2 h and sifted with a 100-mesh sieve to obtain the fine powder.

2.2. Procedures

The procedure was divided into three steps, (i) wet-stirred milling, (ii) alkaline leaching, and (iii) AlN determination (Fig. 2). Wet-stirred milling experiments were carried out at room temperature in a 1L vertical mixing mill containing zirconia balls. The stirring speed was maintained at 400 rpm via use of an electric stirrer (Tianchuang, JMM-1L) and the liquid-solid mass ratio was fixed at 1. At set intervals samples of slurry (30 mL) were taken to examine the size distribution. After wet-stirred milling, the slurry was filtered, washed and transferred to alkaline leaching. The leachate, which contained salts of NaCl, KCl, and NaF was recycled during this process.

Alkaline leaching tests were performed in a 0.5 L glass reactor with a condenser attached to prevent evaporation. Depending upon the specific liquid to solid mass ratio, the filter cake was mixed with NaOH solution maintained at a specified temperature. The stirring speed was held at 300 rpm for the duration of the experiment. Gases (NH_3) evolved from the solution were absorbed by hydrochloric acid connected to the top of the condenser via a pipe. After hydrolysis, the pulp was filtered using a Buchner funnel (#1 Whatman filter paper).

Following this, the AlN content of samples was determined using Kjeldahl methodology [27, 28]. Approximately 1.0 g of dried slurry was weighed and added into a conical flask containing 250 mL of 20% NaOH solution. The solution was boiled for 3 h to evaporate ammonia present. Simultaneously, the ammonia liberated was collected in a 2.5% boric acid solution. The concentration of nitride in the boric acid solution was determined by a hydrochloric acid titration using methyl red/methylene blue as an indicator.

The AlN content in the samples can be calculated using the following equation:

$$C_{AlN} = 0.041 C_{HCl} \cdot (V_1 - V_0)/M \quad (1)$$

where C_{AlN} is the content of AlN in the sample, C_{HCl} is the concentration of HCl, V_1 and V_0 are the volume (ml) of HCl used when the titrating the H_3BO_3 absorbing solution and blank experiment, respectively, and

M is the mass of the sample.

The results obtained from the above experiment were used to calculate the efficiency of AlN removal using the following formula:

$E=(C_0-C_A)*100\%/C_0$ (2)

Where E is the removal efficiency of AlN, C_0 and C_A are the content of AlN in SAD before and after hydrolysis, respectively.

2.3. Analytical methods

The Particle Size Distribution (PSD) of slurry samples were determined using a Malvern Mastersizer 3000 Hydro EV laser diffraction (Malvern, UK). The samples and the residues were characterized by X-ray diffraction (XRD) (D8 advance, Bruker Inc. Germany) employing Cu Kα radiation (35 kV and 30 mA). During XRD analysis, samples were scanned from 5° to 90° with a 0.02° step size and 0.2 sec/step scan speed. The elemental composition of raw materials and residues was determined by X-ray fluorescence (XRF) (Philips, PW 1480, Netherlands) spectrometer with a dual anode Sc/Mo 100 kV 3 kW X-Ray tube. The morphology and composition of the samples and residues were analyzed using a scanning electron microscope (SEM, MLA250, FEI, US) and energy-dispersive X-ray spectroscopy (EDS, MLA250, FEI, US), with both operated at a voltage of 5 kV.

3. Results And Discussions

3.1. Characterization of materials

The chemical composition of prepared SAD is presented in Table 1. The material contained 52.37% Al_2O_3, 18.51% AlN, 7.42% Na_2O and small amounts of other impurities, including Si, Ca, Mg and Fe. XRD analysis of SAD confirmed that the components are primarily Al_2O_3, AlN and other phases like $NaAl_{11}O_{17}$, $MgAl_2O_4$, SiO_2 and NaCl (Fig. 3).

SEM imaging of the SAD sample and the supporting EDS analysis are reported in Fig. 4. Both the shape and particle size of the SAD are irregular (Fig. 4a). SEM investigations demonstrated that nanoparticles were observed to aggregate on the surface of the powder (Fig. 4b). The EDS results demonstrate that these aggregates are primarily Al, O, N containing, likely Al_2O_3 and AlN considering the XRD and chemical composition data.

Table 1
Chemical composition of prepared SAD.

Oxide/element	Al_2O_3	AlN	Na_2O	SiO_2	CaO	MgO	Fe_2O_3
Wt.%	54.37	18.51	7.42	5.77	4.96	2.45	1.37

3.2. wet-stirred milling

To enhance the efficiency of AlN removal from SAD, a wet-stirred milling operation was conducted as a pretreatment before alkaline leaching. It is expected that wet milling would cause a reduction in grain size and assist the hydrolysis of AlN. The effect on size reduction was confirmed by PSD analysis of SAD before, and after, wet-milling (Fig. 5 and Table 2).

Table 2
The distribution values of SAD after different wet-milling time

wet-milling time/min	D_{10}/μm	D_{50}/μm	D_{90}/μm
0	5.01	34.10	150.00
5	2.53	9.20	32.00
10	2.31	5.79	16.20
15	2.28	5.21	15.30

It is observed that the wet-stirred milling operation altered the PSD of SAD, with the particle size of SAD quite sensitive to the milling time. The D_{50} and D_{90} particle sizes of the SAD powder without wet-stirred milling were measured to be 34.1μm and 150μm, respectively. The particle size sharply decreased with increasing milling time up to 10 min. The D_{50} and D_{90} particle sizes of SAD after 10-min wet milling decreased to 5.79 μm and 16.2 μm, respectively. The PSD of SAD became more uniform with an increase in milling time. However, the PSD results didn't change significantly with further increase of milling time from 10 min to 15 min.

Salts present, such as NaCl, KCl, and NaF were dissolved during the wet-milling process. The filtrate was evaporated to obtain the salts, so it could be verified that soluble salts, such as NaCl, KCl, and NaF, were dissolved during the milling process. XRD analysis of the evaporated salts was undertaken (Fig. 6). Removal of these salts assists to reduce the hazardous components and increase the resource recovery from SAD.

3.3. AlN hydrolysis utilizing alkaline leaching

3.3.1 Effect of wet milling time

After wet-stirred milling, SAD was leached in a solution of NaOH. Hydrolysis experiments were performed with 5% NaOH solution and different wet milling times. The efficiency of AlN removal as a function of the milling time at a temperature of 75°C and a S/L mass ratio of 2 is reported in Fig. 7a.

It can be observed that the wet-stirred milling time had significant impact on the efficiency of AlN removal. In comparison, in the experiment without wet-stirred milling, AlN removal efficiency was

depressed. The AlN removal efficiency without wet milling was 83.6% after 120 min and 85.2% at 240 min. As the milling time was increased to 10 min, the AlN removal efficiency reached 98.3% at 120 min, where it remained stable until 240 min, indicating a shorter reaction time to equilibrium. When the wet milling time was increased to 15 min, the AlN removal efficiency declined slightly. Based on these results, the wet-stirred milling time was optimized at 10 min.

The effect of wet-stirred milling on the enhancement of AlN hydrolysis is proposed to be function of grain size reduction. Through reducing the grain size and increasing the active surface contact area, SAD is activated by wet-stirred milling. As salts are mostly dissolved during the milling process, the contact between AlN and the lixiviant will also be improved.

3.3.2 Effect of NaOH addition

The effect of NaOH addition on AlN hydrolysis was investigated (Fig. 7b), displaying the relationship between NaOH concentration and the removal efficiency of AlN after 10 min wet milling, at a leaching temperature of 75°C and a L/S mass ratio of 2.

In comparison to alkaline leaching, water leaching had a reduced AlN hydrolysis reaction, leaching 84.7% of AlN after 120 min. When the NaOH addition amount was increased to 2.5 and 5 wt.%, the removal efficiency increased to 91.2% and 98.3% at 120 min, respectively. When the NaOH concentration was increased to 7.5 wt.%, the AlN removal efficiency reached a plateau, with minimal additional hydrolysis resulting from this further increase. Consequently, the optimal NaOH concentration was 5 wt.% for AlN hydrolysis by alkaline leaching under the experimental conditions.

The impact of NaOH addition can be rationale by the hydrolysis products, AlOOH and $Al(OH)_{3,}$ being readily solubilized by NaOH. This would result in exposing the reactive unhydrolyzed AlN, allowing close to complete leaching during the hydrolysis reaction [29].

3.3.3 Effect of temperature during leaching

The effect of leaching temperature on AlN hydrolysis was evaluated during alkaline leaching experiments. Figure 7(c) reveals the relationship between the removal efficiency of AlN and the leaching temperature. Other experimental conditions are as follows: a wet milling time of 10 min, a concentration of NaOH solution of 5 wt.%, a liquid-to-solid ratio of 2.

The temperature is well known to be an important factor during the hydrolysis of AlN [30]. At temperatures of 25 and 50°C, only 77.8 and 90.7% of AlN were hydrolyzed after 240 min. The removal efficiency of AlN reached a maxima after 120 min at temperatures of 75°C and 100°C, 98.3 and 98.1%, respectively. As evaporation was excessive at 100°C, the optimal temperature for alkaline leaching was determined as 75°C.

From the results shown in Fig. 7, it is concluded that the optimal conditions are wet-stirred milling for 10 min, at a temperature of 75°C and a concentration of NaOH solution of 5 wt.%, with a liquid-to-solid ratio of 2. Under these conditions the efficiency of AlN removal reached 98.3% after 120 min.

3.4. Kinetics of AlN hydrolysis by alkali leaching

Hydrolysis of AlN in NaOH solution is a typical liquid-solid reaction. The morphology and chemical analysis of the slag demonstrate that the hydrolysis reaction can be described by a shrinking core model. In these situations, the reaction rate is typically controlled by either solid layer diffusion or a chemical reaction at the particle surface.

If the reaction rate is determined or limited by diffusion through a solid layer control process, the reaction rate should follow Eq. (3).

$1-2/3X-(1-X)^{2/3}=k_dt$ (3)

If the reaction rate is chemically controlled process, the reaction rate should conform to Eq. (4).

$1-(1-X)^{1/3}=k_rt$ (4)

If the reaction rate is controlled by both diffusion and chemical processes, an integrated rate equation will best describe the data (Eq. 5).

$[ln(1-X)]/3-1+(1-X)^{-1/3}=k_mt$ (5)

Where X is the removal efficiency of AlN, k_d is the kinetic parameter for diffusion through a solid layer control process, k_r is the kinetic parameter for the chemical reaction control process, k_m is the kinetic parameter for a mixed control process and t is the reaction time (min).

The alkali leaching experiments of SAD were performed after a wet-stirred milling of 10 min, at a NaOH concentration of 5 wt.% and a liquid-to-solid ratio of 2, at different temperature and time to determine the reaction rate controlling step. The experimental data were fitted using Eqs. (3), (4) and (5), with the results reported in Figs. 8(a), (b) and (c).

It is evident that there is a strong linear relationships and elevated correlation coefficient (R^2) in Fig. 8(c), indicating that the data was best fitted by the mixed process control model. In comparison, the experimental data didn't fit diffusion or chemical control models with a high degree of accuracy. Consequently, the data indicates that the hydrolysis process is controlled by both the rates of diffusion and the chemical reaction.

The temperature dependence of the reaction can be calculated using the Arrhenius equation:

$k = Aexp(-E_a/RT)$ (6)

Where A is the frequency factor, E_a is the activation energy of the reaction, R is the universal gas constant, and T is the absolute temperature.

The plot of lnk with respect to 1000/T is reported over the temperature range of 25 ~ 100°C to evaluate the activation energy of the hydrolysis process (Fig. 8d). The slope ($-E_a/R$), and the activation energy were calculated to be 31 kJ/mol. This result is consistent with typical reported apparent activation energies in mixed control processes[27].

3.5. Product characterization

XRD, XRF and SEM-EDS were undertaken to characterize the residue of the hydrolysis process under optimal conditions. XRD results demonstrated peaks characteristic of Al_2O_3 and $Al(OH)_3$ were present, while the typical signal of AlN is completely lost (Fig. 9). Some weak signals present correspond to the presence of low-content compounds, such as $NaAl_{11}O_{17}$, $MgAl_2O_4$ and SiO_2. The chemical composition of SAD after hydrolysis is reported in Table 3 and in consistent with the XRD results.

SEM analysis (Fig. 10) demonstrates that after hydrolysis a large number of hexagonal nano-particles (with an average diameter of 200 nm) are present over the particle surface. Similar phenomena have been widely found during the hydrolysis of AlN powder [23]. EDS results for SAD after hydrolysis report only the presence of elemental O and Al in these particles (Fig. 10).

Therefore, the XRF, XRD, and SEM-EDS analysis confirmed that the combination of wet-stirred milling and alkaline leaching effectively removed AlN from SAD. The hydrolysis residue consists primarily of Al_2O_3 and $Al(OH)_3$, allowing it to be recycled as an Al concentrate.

Table 3
Chemical composition of SAD after hydrolysis.

Oxide/element	Al_2O_3	Na_2O	SiO_2	CaO	MgO	Fe_2O_3
Wt.%	81.52	1.7	5.19	5.29	4.45	1.12

4. Conclusions

An enhanced hydrolysis process for removing AlN from SAD has been developed and reported in this study. The results demonstrate that the progress is highly efficient and can be performed using a combination of wet-stirred milling and alkaline leaching. SAD is activated by wet-stirred milling with water by reducing the grain size and increasing the active contact area. Alkaline leaching can dissolve the hydrolysis products to expose the reactive sites of unhydrolyzed AlN, allowing enhanced hydrolysis to take place.

Under the optimum conditions, the removal efficiency of AlN reached 98.3%. The leachate can be recycled as a lixiviant, with the residues used as Al concentrate. The process is efficient and comparatively environmentally friendly for the removal of AlN from SAD. The technology has been already applied in a pilot plant that processes 20000 tons of SAD per year, achieving a favorable effect in practical applications, facilitating the disposal of waste and the protection of environment.

Declarations

Acknowledgements

This work was financially supported by National key Technologies R&D Programs (NO.2020YFC1909601, NO.2020YFC1909603), and Natural Science Foundation of Hebei Province (NO. E2020111205). The authors wish to thank these organizations for their continued support throughout the course of the project. The authors also would like to express their gratitude to EditSprings (https://www.editsprings.com/) for the expert linguistic services provided.

Statements & Declarations

This work was financially supported by National key Technologies R&D Programs (NO.2020YFC1909601, NO.2020YFC1909603), and Natural Science Foundation of Hebei Province (NO. E2020111205). The authors have no relevant financial or non-financial interests to disclose.

Data Availability Statement

The datasets generated during and/or analysed during the current study are not publicly available due to individual privacy, but are available from the corresponding author on reasonable request.

References

1. Meshram, A., Singh, K.K.: Recovery of valuable products from hazardous aluminum dross: A review. Resour. Conserv. Recycl. **130**, 95–108 (2018)
2. Hu, K., Reed, D., Robshaw, T.J., Smith, R.M., Ogden, M.D.: Characterisation of aluminium black dross before and after stepwise salt-phase dissolution in non-aqueous solvents. J. Hazard. Mater. **401**, 123351 (2021)
3. El-Katatny, E.A., Halawy, S.A., Mohamed, M.A., Zaki, M.I.: Recovery of high surface area alumina from aluminium dross tailings. J. Chem. Technol. Biotechnology: Int. Res. Process Environ. Clean Technol. **75**, 394–402 (2000)
4. Mahinroosta, M., Allahverdi, A.: A promising green process for synthesis of high purity activated-alumina nanopowder from secondary aluminum dross. J. Clean. Prod. **179**, 93–102 (2018)
5. How, L.F., Islam, A., Jaafar, M.S., Taufiq-Yap, Y.H.: Extraction and Characterization of γ-Alumina from Waste Aluminium Dross, Waste and Biomass Valorization, 8321–327. (2017)
6. Yang, S.F., Wang, T.M., Shie, Z.Y.J., Jiang, S.J., Hwang, C.S., Tzeng, C.C.: Fine Al_2O_3 powder produced by radio-frequency plasma from aluminum dross. IEEE Trans. Plasma Sci. **42**, 3751–3755 (2014)
7. David, E., Kopac, J.: Aluminum recovery as a product with high added value using aluminum hazardous waste. J. Hazard. Mater. **261**, 316–324 (2013)

8. Mailar, G., Raghavendra, S., Sreedhara, B., Manu, D., Hiremath, P., Jayakesh, K.: Investigation of concrete produced using recycled aluminium dross for hot weather concreting conditions. Resource-Efficient Technol. **2**, 68–80 (2016)
9. Inseemeesak, B., Rodchanarowan, A.: The influence of aluminium dross on cement paste's porosity,Advanced Materials Research, Trans Tech Publ, pp.445–448. (2013)
10. Dai, C., Apelian, D.: Fabrication and characterization of aluminum dross-containing mortar composites: upcycling of a waste product. J. Sustainable Metall. **3**, 230–238 (2017)
11. Tsakiridis, P.E., Oustadakis, P., Agatzini-Leonardou, S.: Black dross leached residue: an alternative raw material for portland cement clinker, Waste and Biomass Valorization, 5973–983. (2014)
12. Yoshimura, H.N., Abreu, A.P., Molisani, A.L., de Camargo, A.C., Portela, J.C.S., Narita, N.E.: Evaluation of aluminum dross waste as raw material for refractories. Ceram. Int. **34**, 581–591 (2008)
13. Li, A., Zhang, H., Yang, H.: Evaluation of aluminum dross as raw material for high-alumina refractory. Ceram. Int. **40**, 12585–12590 (2014)
14. Murayama, N., Okajima, N., Yamaoka, S., Yamamoto, H., Shibata, J.: Hydrothermal synthesis of AlPO4-5 type zeolitic materials by using aluminum dross as a raw material. J. Eur. Ceram. Soc. **26**, 459–462 (2006)
15. Kim, J., Biswas, K., Jhon, K.W., Jeong, S.Y., Ahn, W.S.: Synthesis of AlPO4-5 and CrAPO-5 using aluminum dross. J. Hazard. Mater. **169**, 919–925 (2009)
16. Perego, C., Bagatin, R., Tagliabue, M., Vignola, R.: Zeolites and related mesoporous materials for multi-talented environmental solutions. Microporous Mesoporous Mater. **166**, 37–49 (2013)
17. Zhang, Y., Li, S., Wang, X., Li, X.: Coagulation performance and mechanism of polyaluminum ferric chloride (PAFC) coagulant synthesized using blast furnace dust. Sep. Purif. Technol. **154**, 345–350 (2015)
18. Abdulkadir, A., Ajayi, A., Hassan, M.I.: Evaluating the chemical composition and the molar heat capacities of a white aluminum dross. Energy Procedia. **75**, 2099–2105 (2015)
19. Li, P., Guo, M., Zhang, M., Teng, L., Seetharaman, S.: Leaching Process Investigation of Secondary Aluminum Dross: The effect of CO_2 on leaching process of salt cake from aluminum remelting process. Metall. Mater. Trans. B. **43**, 1220–1230 (2012)
20. Hao, L., Wei, H.: On-line investigation of anatase precipitation from titanyl sulphate solution. Chem. Eng. Res. Des. **88**, 1264–1271 (2010)
21. Zhang, Y., Guo, Z., Han, Z., Xiao, X., Peng, C.: Feasibility of aluminum recovery and MgAl 2 O 4 spinel synthesis from secondary aluminum dross. Int. J. Minerals Metall. Mater. **26**, 309–318 (2019)
22. Li, Q., Yang, Q., Zhang, G., Shi, Q.: Investigations on the hydrolysis behavior of AlN in the leaching process of secondary aluminum dross, Hydrometallurgy, 182 121–127. (2018)
23. Kocjan, A.: The hydrolysis of AlN powder-A powerful tool in advanced materials engineering. Chem. Record. **18**, 1232–1246 (2018)

24. Kocjan, A., Dakskobler, A., Kosmač, T.: Evolution of aluminum hydroxides in diluted aqueous aluminum nitride powder suspensions. Cryst. Growth. Des. **12**, 1299–1307 (2012)
25. Guo, Q., Li, Y.L., Liu, Y.F., Qi, T.: A kind of deep hydrolysis method of aluminum nitride in aluminum dross. CN108217688 B, CN patent NO (2021)
26. Fu, M.B., Guo, Q., Li, Y.L., Tian, D.C.: A kind of method for strengthening aluminum dross desalination and denitrification. CN110314923 B, CN patent NO (2021)
27. Wagner, E.: Titration of ammonia in presence of boric acid. Industrial & Engineering Chemistry Analytical Edition. **12**, 771–772 (1940)
28. Meeker, E.W., Wagner, E.: Titration of ammonia in presence of boric acid. Industrial & Engineering Chemistry Analytical Edition. **5**, 396–398 (1933)
29. Lv, H., Zhao, H., Zuo, Z., Li, R., Liu, F.: A thermodynamic and kinetic study of catalyzed hydrolysis of aluminum nitride in secondary aluminum dross. J. Mater. Res. Technol. **9**, 9735–9745 (2020)
30. Fukumoto, S., Hookabe, T., Tsubakino, H.: Hydrolysis behavior of aluminum nitride in various solutions. J. Mater. Sci. **35**, 2743–2748 (2000)

Figures

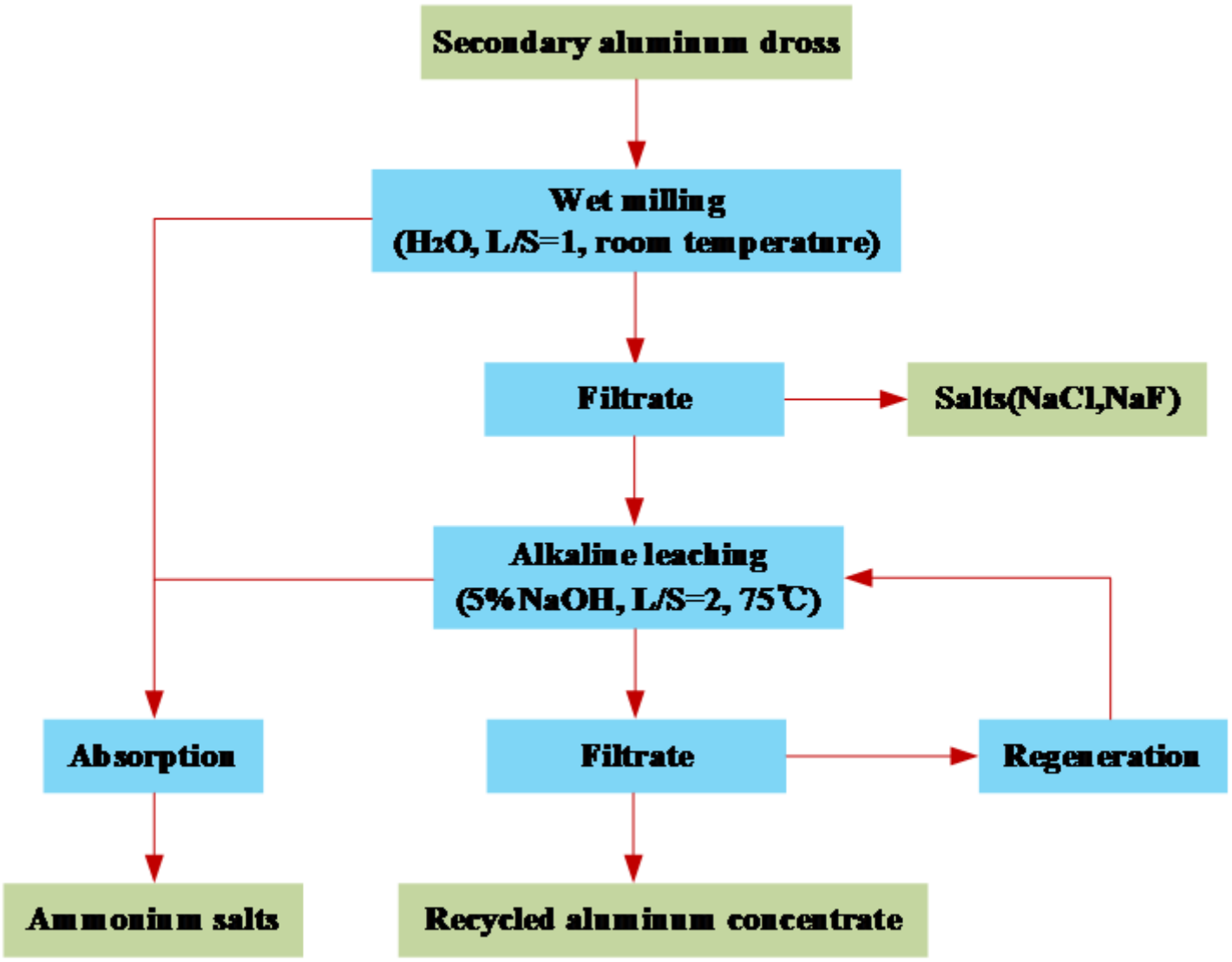

Figure 1

Proposed flow-sheet for the hydrolysis of AlN from SAD.

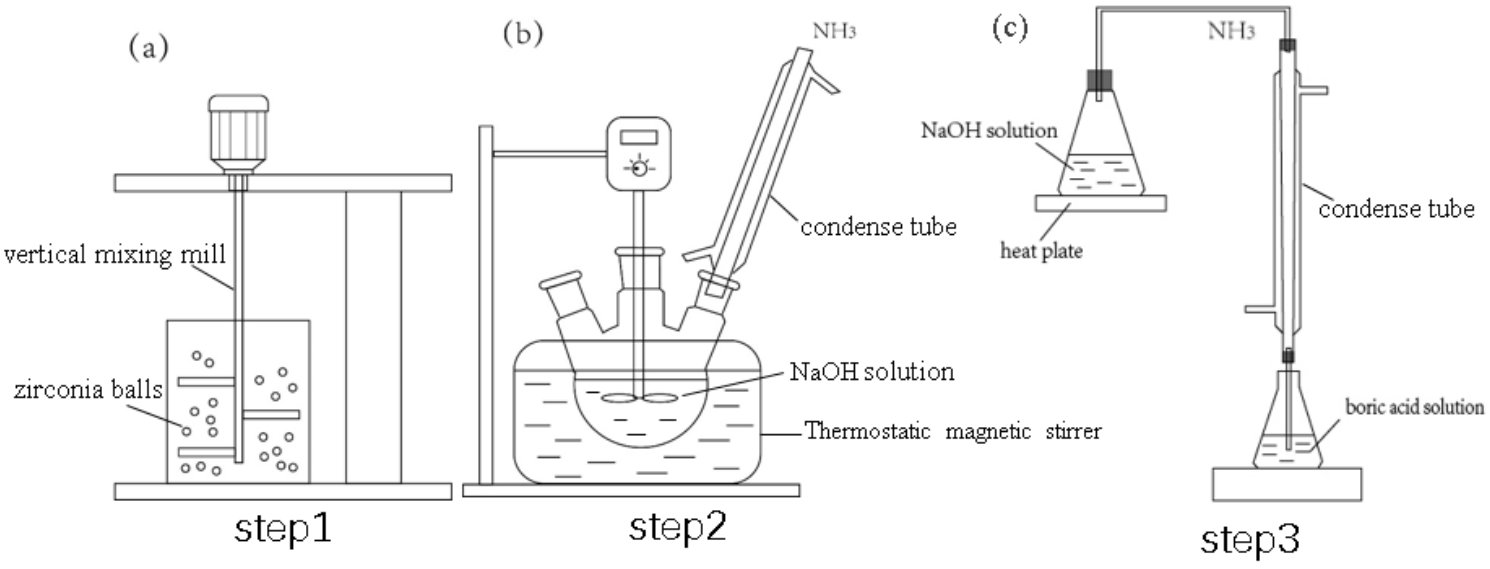

Figure 2

Schematic experimental setup and procedure (a) wet-stirred milling, (b) alkaline leaching, (c) AlN determination.

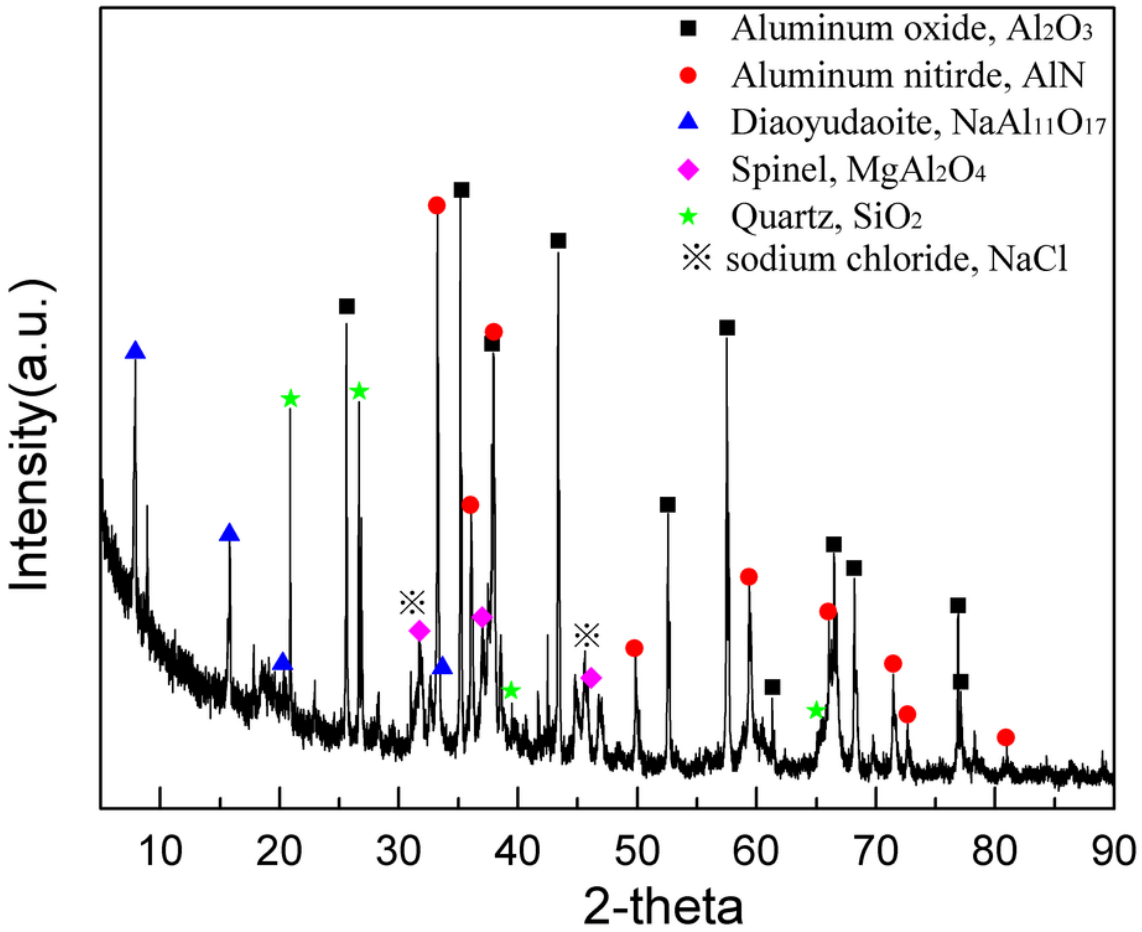

Figure 3

X-ray powder diffraction analysis of SAD

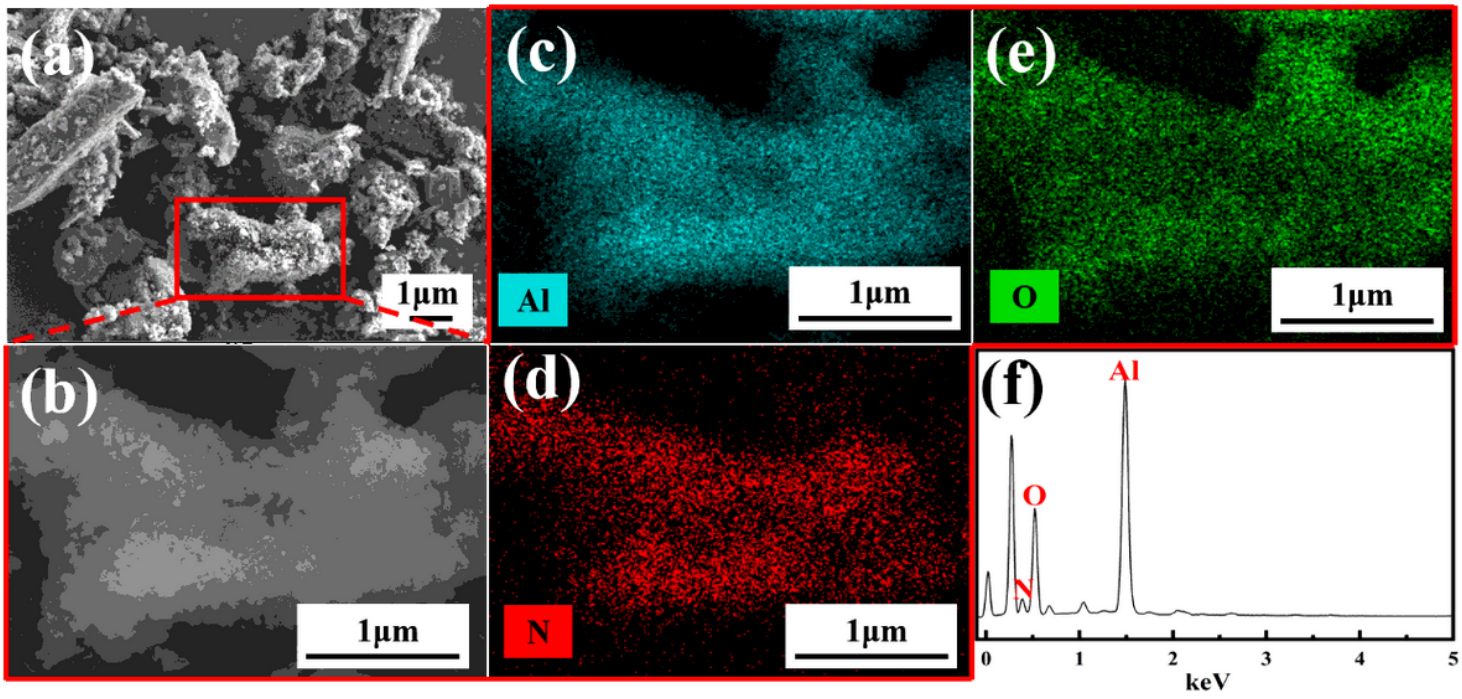

Figure 4

(a,b). SEM images of SAD and (c, d, e, f). EDS analysis for the region shown in(a).

3.2. wet-stirred milling

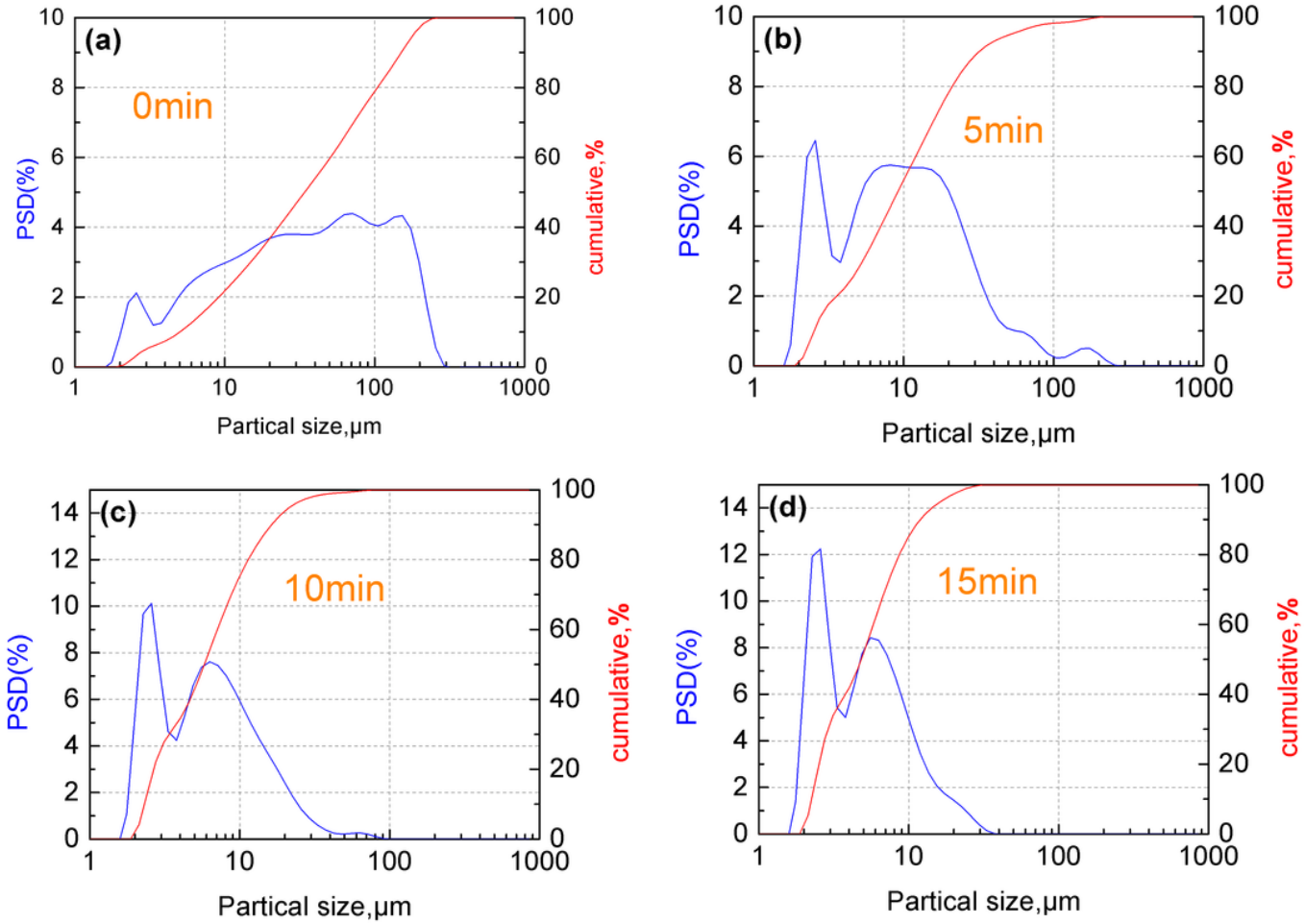

Figure 5

Particle size distribution of SAD after wet milling for (a) 0 min; (b) 5min; (c) 10 min; (d) 15 min. The curves referring to the left hand y-axis indicate the percentage of particles by PSD class. The right hand y-axis refers to the cumulative PSD.

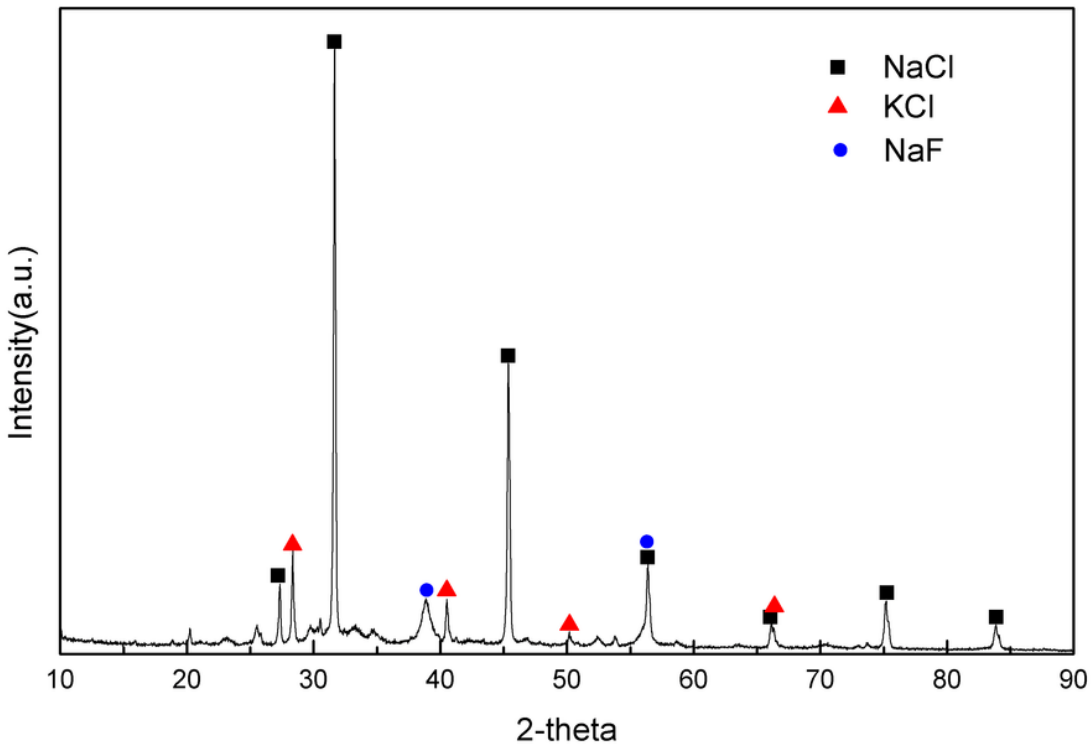

Figure 6

XRD pattern of the vaporized salts.

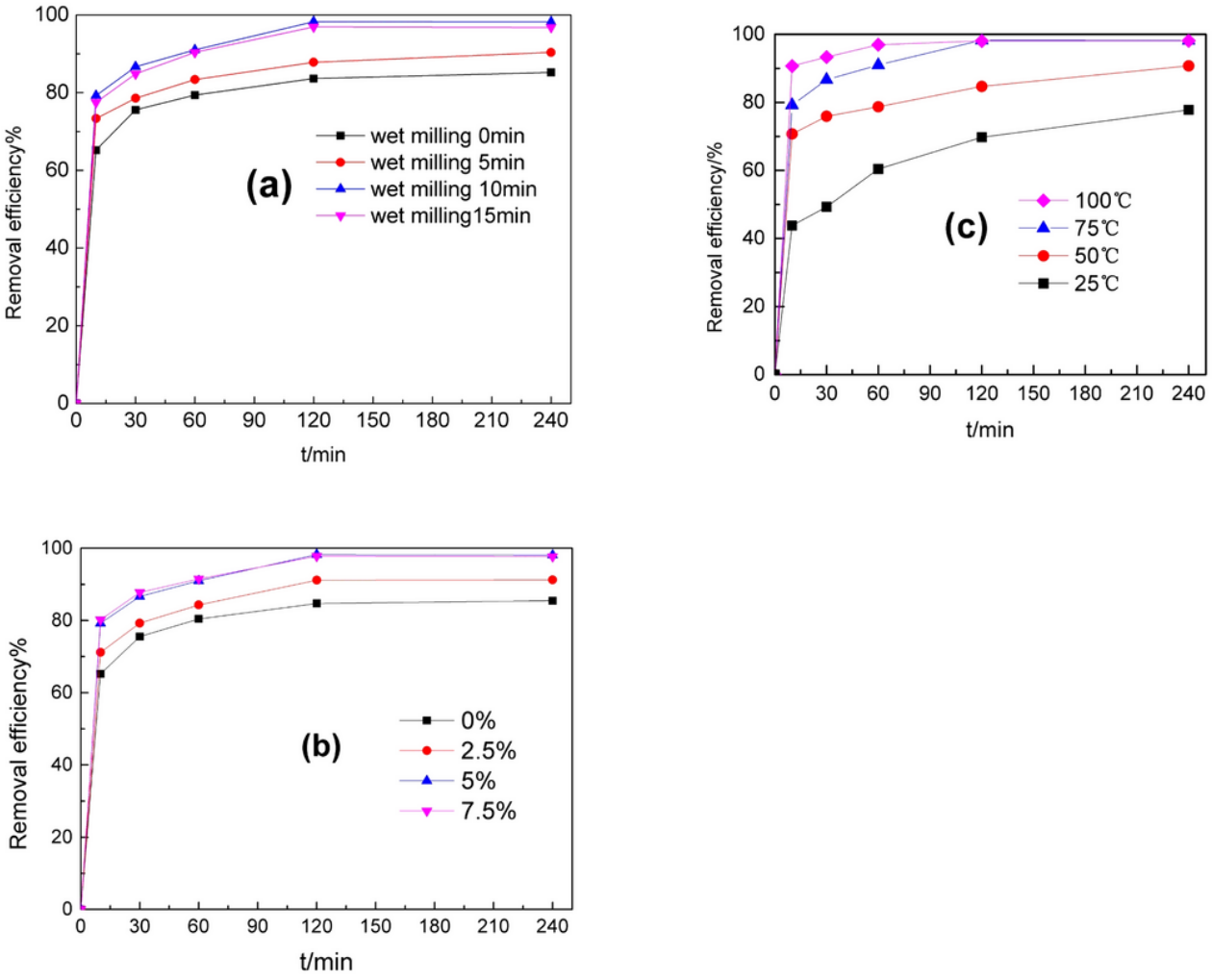

Figure 7

The effect of hydrolysis conditions (a) wet milling time, (b) concentration of NaOH, (c) leaching temperature on theefficiency of AlN removal from SAD.

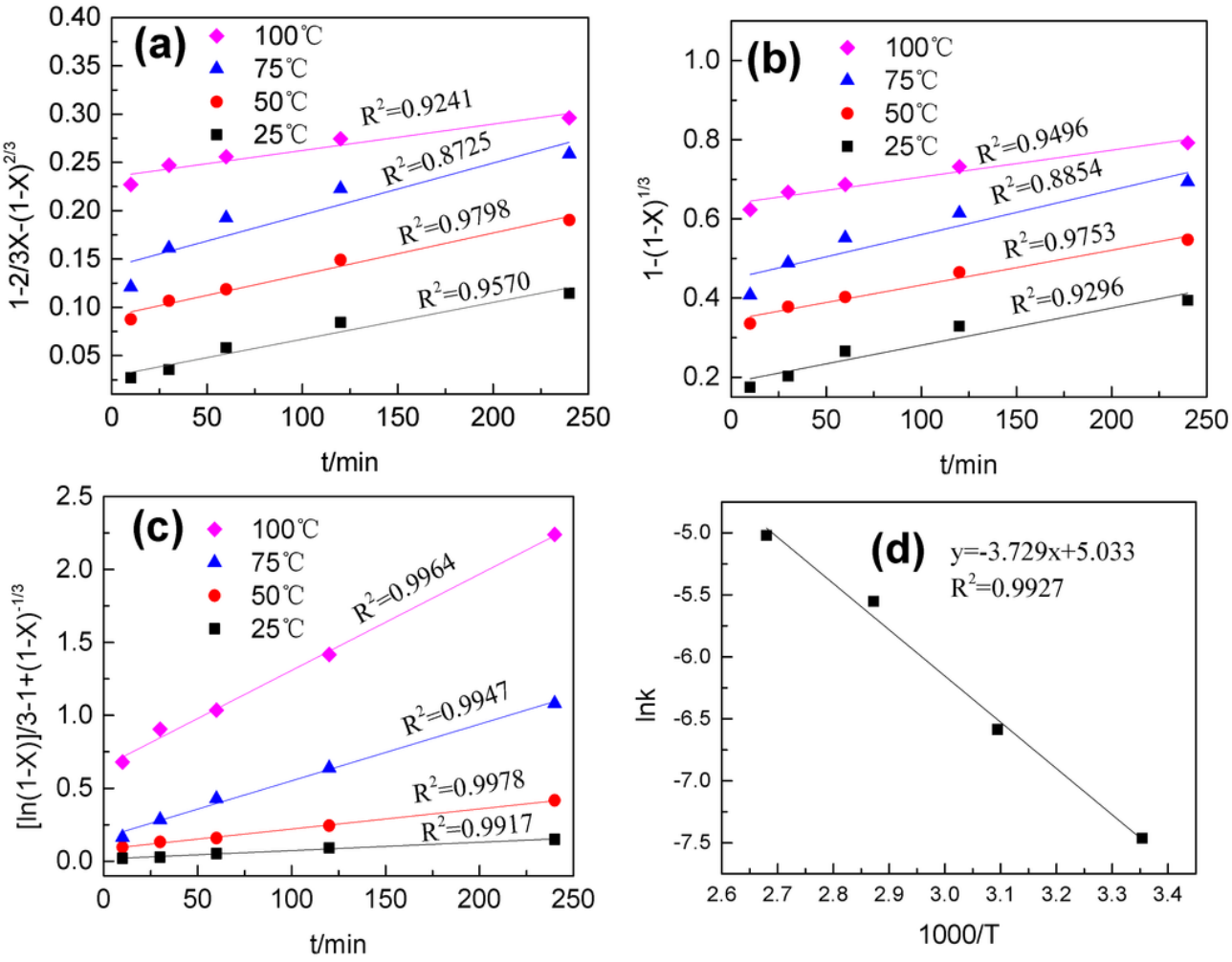

Figure 8

The plot of (a) $1-2/3X-(1-X)^{2/3}$; (b) $1-(1-X)^{1/3}$; (c) $[\ln(1-X)]/3-1+(1-X)^{-1/3}$ against the time at different temperatures (d) Relationship between lnk and 1000/T

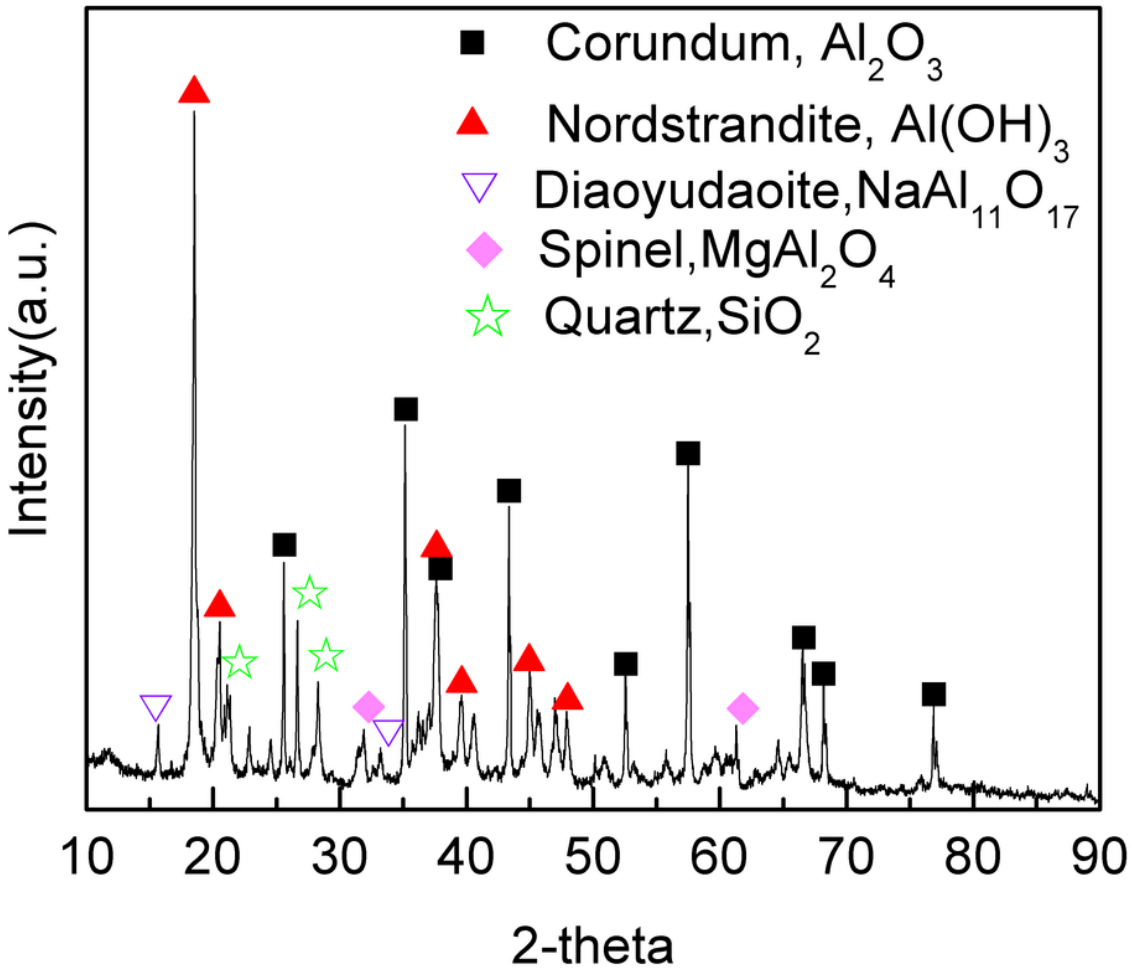

Figure 9

XRD analysis of SAD afterhydrolysis

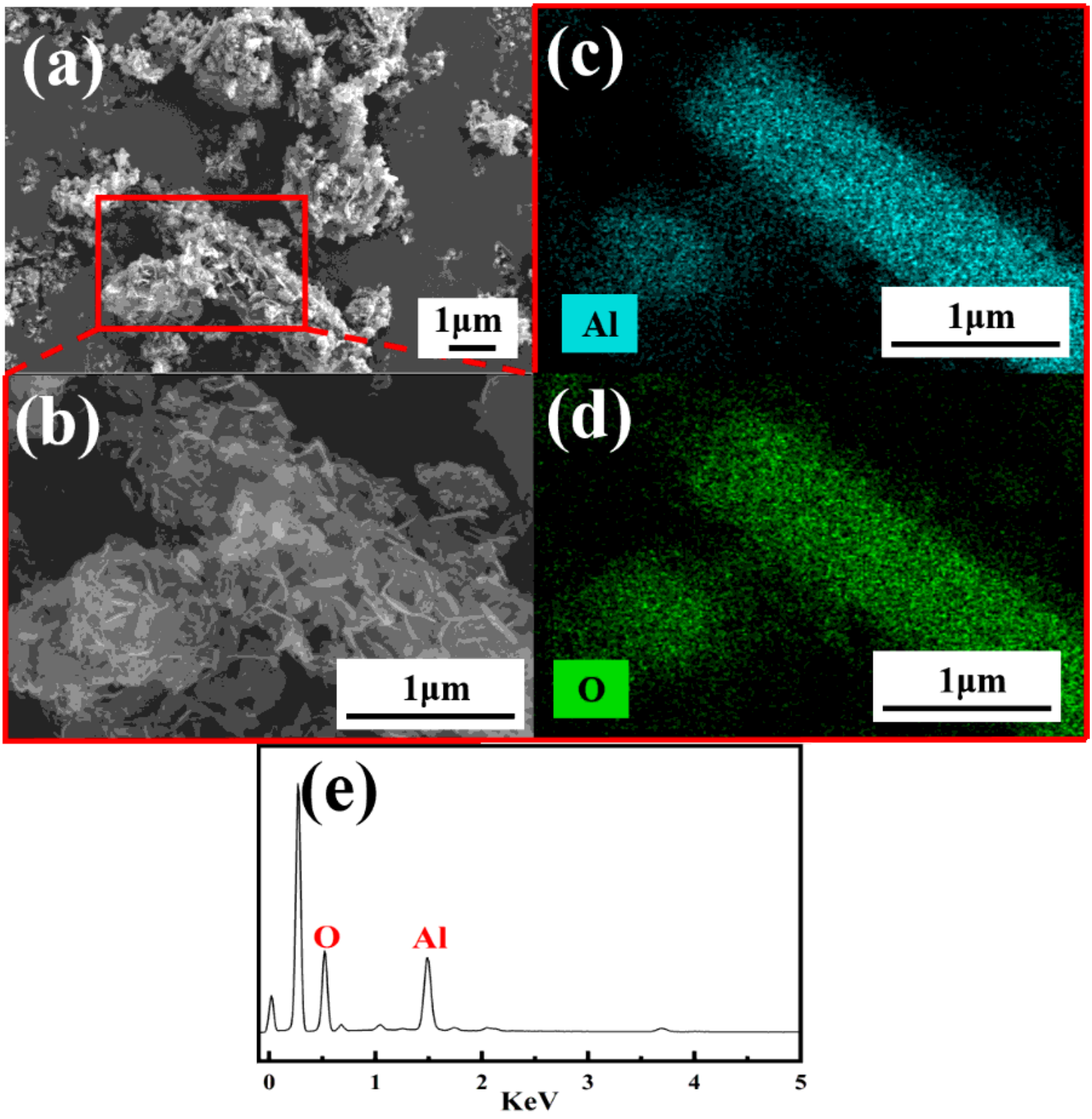

Figure 10

(a,b). SEM images for SAD after hydrolysis and (c, d, e). EDS analysis of the region presented in (a).